Enhanced Corrosion Protection Coatings Prepared from Soluble Electronically Conductive Polypyrrole-Clay Nanocomposite Materials

Jui-Ming Yeh, Chih-Ping Chin, Susan Chang

Department of Chemistry and Center for Nanotechnology at CYCU, Chung-Yuan Christian University, Chung Li, Taiwan 320, Republic of China

Received 29 April 2002; accepted 19 September 2002

ABSTRACT: A series of electronically conductive nanocomposite materials that consisted of soluble polypyrrole (PPY) and layered montmorillonite (MMT) clay platelets were prepared by effectively dispersing the inorganic nanolayers of MMT clay in organic PPY matrix via an *in situ* oxidative polymerization with dodecylbenzene sulfonic acid (DBSA) as dopant. Organic pyrrole monomers were first intercalated into the interlayer regions of organophilic clay hosts and followed by a one-step oxidative polymerization. The as-synthesized electronically conductive polypyrrole–clay nanocomposite (PCN) materials were then characterized by Fourier transformation infrared (FTIR) spectroscopy, wide-angle powder X-ray diffraction (XRD), and transmission electron microscopy (TEM). PCNs in the form of coatings with low clay loading (e.g., 1.0 wt %) on cold-rolled steel (CRS) were found to exhibit much better in corrosion protection over those of pristine PPY based on a series of electrochemical measurements including corrosion potential, polarization resistance, and corrosion current in 5 wt % aqueous NaCl electrolyte. Effects of the material composition on the thermal stability, optical properties, and electrical conductivity of pristine PPY along with PCN materials, in the form of fine powder, powder-pressed pellet, and solution, were also studied by differential scanning calorimetry (DSC), thermogravimetric analysis (TGA), UV-visible absorption spectra, and four-point probe technique, respectively. The viscosity of PPY existed in PCN materials and pristine PPY were determined by viscometric analysis with *m*-cresol as solvent. The heterogeneous nucleating effect of MMT clay platelets in PPY matrix was studied by wide-angle powder XRD. The corresponding morphological images of the nucleating behavior of clay platelets in PPY matrix were investigated by scanning electron microscopy (SEM). © 2003 Wiley Periodicals, Inc. J Appl Polym Sci 88: 3264–3272, 2003

Key words: clay; conjugated polymers; coatings

INTRODUCTION

Layered materials, such as smectite clays (e.g., montmorillonite, MMT), evoked a great amount of attention for the preparation of various novel polymer–clay nanocomposite (PCN) materials lately, because their lamellar structures had high in-plane strength and stiffness as well as a high aspect ratio.[1] The PCN materials were found to exhibit advanced gas barrier,[2] thermal stability,[3] mechanical strength,[4] and fire-retardant[5] properties compared to pristine polymers. There was much published literature focused on the preparation and new property studies of the novel nanocomposites consisting of conducting polymer with various layered materials.[6–12]

Generally, conducting polymers consisted of conjugated electronic structures and are conventionally classified into three main groups: aromatic hydrocarbons (e.g., polyaniline), heterocyclics (e.g., polythiophene, polypyrrole, PPY), and aliphatic hydrocarbons (e.g., polyacetylene). They have received considerable attention recently because of many promising technological applications. For example, some specific conducting polymers, such as polyaniline and its derivatives, had been found to display interesting corrosion protection properties. In the past decade, polyaniline as anticorrosion coatings had been explored to be potential candidates used to replace the chromium-containing materials, which have negative health and environmental concerns.[13–18] Wei et al.[18] showed the corrosion protection effect of polyaniline coatings through a series of electrochemical measurements on the doped or undoped polyaniline-coated cold-rolled steel (CRS) under various conditions. Wessling[17] proposed a full mechanism by which the anticorrosion performance of polyaniline on steel was attributed to an increase in the corrosion potential and to the redox catalytic property of polyaniline in the formation of a passive layer of metal oxide. On the other hand, corrosion protection of electroactive heterocyclic polypyrrole had also attracted extensive research interest in the recent decade.[19–20]

Correspondence to: J.-M. Yeh (juiming@cycu.edu.tw).

Contract grant sponsor: NSC; contract grant number: 90-2113M-033-010.

Journal of Applied Polymer Science, Vol. 88, 3264–3272 (2003)

Recently, we found that the dispersion of MMT clay platelets into various polymeric matrices [e.g., polyaniline,[21] poly(*o*-etnoxyaniline),[22] and poly(methyl methacrylate)[23]] can effectively enhance the corrosion protection effect of pristine polymers on CRS coupons based on a series of electrochemical corrosion measurements in saline. We also noted that some research groups reported the preparation and property studies focused on poly(heterocyclics)–clay nanocomposites such as poly(thiophene)–clay[24] and polypyrrole–clay.[24,25] However, the corrosion protection effect of polypyrrole–clay nanocomposite coatings has never been mentioned. Therefore, in this article, we will present the first evaluation of corrosion protection effect for the soluble electronically conductive polypyrrole–clay nanocomposite materials on CRS in comparison with that of pristine electronically conductive polypyrrole by performing a series of electrochemical measurements of corrosion potential, polarization resistance, and corrosion current in 5 wt % aqueous NaCl electrolyte. Subsequently, PCN materials were characterized by Fourier transform infrared (FTIR) spectroscopy, wide-angle powder X-ray diffraction (WAXRD), and transmission electron microscopy (TEM). The effect of material composition on thermal stability, optical properties, electrical conductivity of electronically conductive polypyrrole, along with PCN materials, in the form of fine powder, powder-pressed pellet, and solution, were also studied by differential scanning calorimetry (DSC), thermogravimetric analysis (TGA), UV-visible absorption spectra, and four-point probe technique, respectively. Viscosity of PPY existed in PCN materials and pristine PPY was determined by viscometric analysis with *m*-cresol as solvent.

The heterogeneous nucleating effect of MMT clay platelets in polymeric matrix was studied by wide-angle powder XRD. The corresponding morphological images of nucleating behavior for clay platelets in composites were also investigated by scanning electron microscopy (SEM).

EXPERIMENTAL

Chemicals and instrumentations

Pyrrole (98%, Fluka) was dried with CaH_2 for 24 h, followed by distillation under reduced pressure. *m*-Cresol (99%, Lancaster), chloroform (J. T. Baker), HCl (37%, Riedel-De Haen), and methanol (Riedel-De Haen) were used as received without further purification. Ammonium persulfate (APS) (98%, Merck) and dodecylbenzene sulfonic acid (DBSA, TCI) were functioned as oxidant and acid dopant, respectively. The montmorillonite clay employed in this study was PK 805 with a cationic exchange capacity (CEC) value of 98 mequiv/100 g supplied by Pai-Kong Ceramic Co., Taiwan. The structure of intercalating agent was $C_{11}H_{23}CONH(CH_2)_2N^+(CH_3)_2CH_2CHOHCH_2SO_3^-$ (cocamidopropylhydroxysultaine) provided by Industrial Technology Research Institute (ITRI), Taiwan.

Wide-angle X-ray diffraction pattern of the samples was carried out on a Rigaku D/MAX-3C OD-2988N X-ray diffractometer with a cooper target and a Ni filter at a scanning rate of 4°/min. The samples for the TEM study was first prepared by putting powder of PCN materials into epoxy resin capsules, followed by curing the epoxy resin at 100°C for 24 h in a vacuum oven. Subsequently, the cured epoxy resin containing PCN materials were microtomed with a Reichert-Jumg Ultracut-E into 60- to 90-nm-thick slices. Then, one layer of carbon about 10 nm thick was deposited on these slices on 100-mesh copper nets for TEM observations on a JEOL-200FX with an acceleration voltage of 120 kV.

Electrochemical measurements of sample-coated CRS coupons were performed on a VoltaLab 21 Potentiostat/Galvanostat in a standard corrosion cell equipped with two graphite rod counter electrodes and a saturated calomel electrode (SCE) as well as the working electrode. A Perkin–Elmer thermal analysis system equipped with a model 7 DSC and a model 7/DX TGA were employed for the thermal analyses under air or nitrogen flow. The programmed heating rate was 20°C/min in most cases. FTIR spectra were recorded on pressed KBr pellets by using a Bio-Rad FTS-7 FTIR spectrometer. The UV-visible absorption spectra of a very dilute solution of the polymer in *m*-cresol were recorded on a Hitachi U-2000 UV-visible spectrometer at room temperature. The viscosity data of polymer in *m*-cresol solution were obtained with a Schott Avs 310-type viscometer at 24 ± 1°C. Conductivity measurements were made on a four-point probe connected to a Keithley 2400 voltmeter constant-current source system. The morphology of polymer was examined on a JEOL JSM-6330F SEM.

Synthesis of electronically conductive polypyrrole

As a typical procedure, both 24.3 g (0.15 mol) DBSA and 10 g (0.30 mol) pyrrole monomers were dissolved in 400 mL distilled water under vigorous magnetic stirring. An amount of 6.8 g (0.06 mol) of APS as oxidant dissolved in 100 mL of distilled water was subsequently added dropwise to the previous solution, the temperature of which was kept at 5°C. This oxidative polymerization reaction was maintained for 40 h and subsequently terminated by pouring a large amount (e.g., 300 mL) of methanol. PPY was then precipitated from the solution. The crude product was obtained by filtering and washing sequentially with distilled water, methanol, and acetone several times, followed by drying in vacuum at 30°C for 12 h. Elec-

tronically conductive polypyrrole was obtained as a black powder with ~ 38% yield.

Preparation of organophilic clay

Organophilic clay was prepared by a cationic-exchange reaction between the sodium cations of MMT clay and alkylammonium ions of intercalating agent, cocamidopropylhydroxysultaine. Typically, 5 g MMT clay with a CEC value of 98 mequiv/100 g was stirred in 500 mL distilled water (beaker A) at room temperature overnight. A separate solution containing 2.21 g of intercalating agent in another 100 mL of distilled water (beaker B) was magnetically stirred, followed by the addition of 1.0*M* HCl aqueous solution to regulate the pH value approaching ~ 3–4. After stirring for 1 h, the protonated amino acid solution (beaker B) was added at a rate of approximately 10 mL/min with vigorous stirring to the MMT suspension (beaker A). The mixture with stirring was maintained overnight at room temperature. The organophilic clay was recovered by ultracentrifuging (9000 rpm, 30 min) and filtering the solution in a Buchner funnel. Purification of products was performed by washing and filtering samples repeatedly at least three times to remove any excess amount of ammonium ions.

Preparation of electronically conductive polypyrrole–clay nanocomposite materials

As a representative step to prepare the PCN materials with 1 wt % clay loading (i.e., PPYCL1), first, 0.1 g organophilic clay was introduced into 400 mL distilled water under magnetic stirring overnight at room temperature. Pyrrole monomers (10 g, 0.3 mol) and DBSA (24.3 g, 0.15 mol) were subsequently added to the previous solution, which was stirred for another 24 h at 5°C. Upon addition of ammonium persulfate (6.8 g, 0.06 mol) in 100 mL distilled water, the solution was stirred for 40 h at 5°C in an ice bath and then terminated by pouring a large amount (e.g., 300 mL) of methanol. PCN materials were then precipitated from the mixing solution as a black powder, followed by filtering and sequentially washing with distilled water, methanol, and acetone several times. The as-synthesized DBSA-doped nanocomposite precipitates were then obtained by drying under vacuum at 30°C for 12 h.

Preparation of coatings and electrochemical measurements

As a representative procedure for preparing the electronically conductive PPY coatings for electrochemical corrosion measurements, black polypyrrole and PCN fine powder were dissolved in chloroform; an equal amount of DBSA by weight was required to be added to effectively enhance the solubility of polypyrrole in chloroform for making the 1 wt % solutions.[32] After filtering through a Teflon membrane with a pore size of 1 μm, the solution was then dip-coated onto CRS coupons (1.0 × 1.0 cm) and followed by drying in air for 12 h to give coatings of ~ 60 μm thickness. The coated and uncoated coupons were subsequently mounted to the working electrode so that only the coated side of the coupon was in direct contact with the electrolyte. The edges of the coupons were sealed with superfast epoxy cement (SPAR®). All electrochemical measurements were performed at room temperature and repeated at least three times. The electrolyte used was NaCl (5 wt %) aqueous solution. The open circuit potential (OCP) at the equilibrium state of the system was recorded as the corrosion potential (E_{corr} in V versus SCE). The polarization resistance (R_p in Ω/cm^2) was measured by sweeping the applied potential from 20 mV below to 20 mV above the E_{corr} at a scan rate of 500 mV/min and recording the corresponding current change. The R_p value was obtained from the slope of the potential-current plot. The Tafel plots were obtained by scanning potential from 250 mV below to 250 mV above the E_{corr} at a scan rate of 500 mV/min. Corrosion current (i_{corr}) was determined by superimposing a straight line along the linear portion of the cathodic or anodic curve and extrapolating it through E_{corr}. The corrosion rate (R_{corr}, in milli-inches per year, MPY) was calculated by the equation:

$$R_{corr}\ (\text{MPY}) = [0.13\ i_{corr}(\text{E.W.})]/[Ad]$$

where EW is the equivalent weight (in g/equiv), A is the area (in cm^2), and d is the density (in g/cm^3).

RESULTS AND DISCUSSION

Smectite clay (e.g., MMT) is a clay mineral containing stacked silicate sheets measuring ~ 10 Å in thickness and ~ 2180 Å in length.[26] It possesses a high aspect ratio and a platey morphology. The typical chemical structures of MMT usually consist of two fused silica tetrahedral sheets sandwiching an edge-shared octahedral sheet of either magnesium or aluminum hydroxide. The Na^+ and Ca^{+2} residing in the interlayer regions can be replaced by organic cations such as alkylammonium ions by an cationic-exchange reaction to render the hydrophilic layered silicate organophilic. MMT has a high swelling capacity, which is important for efficient intercalation of the polymer, and is composed of stacked silicate sheets that offer enhanced thermal stability, mechanical strength, fire retardant, molecular barrier, and corrosion protection properties.

Before synthesizing the PCN materials, organophilic clay was first prepared by a cationic-exchange reaction between the sodium cations of MMT clay and

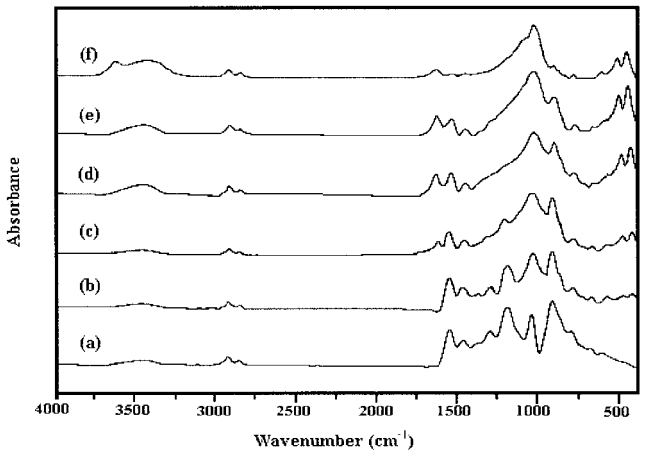

Figure 1 FTIR spectra of (a) PPY, (b) PPYCL1, (c) PPYCL3, (d) PPYCL5, (e) PPYCL10, (f) organophilic clay.

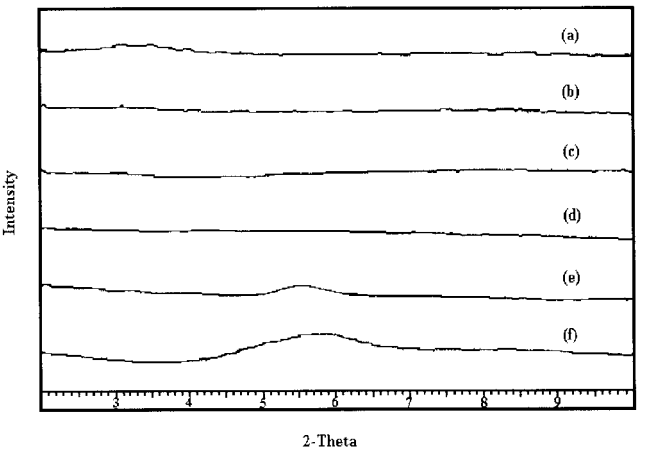

Figure 2 Wide-angle powder X-ray diffraction patterns of (a) PPY, (b) PPYCL1, (c) PPYCL3, (d) PPYCL5, (e) PPYCL10, (f) organophilic clay.

alkylammonium ions of cocamidopropylhydroxysultaine. Organic pyrrole monomers were subsequently intercalated into the interlayer regions of organophilic clay hosts and followed by a one-step oxidative polymerization. The composition of the PCN materials can vary from 0 to 10 wt % of clay with respect to electronically conductive PPY content.

Characterization

The characteristic FTIR spectra of the organophilic clay, pristine PPY, and PCN materials were illustrated in Figure 1. The representative vibration bands of PPY were at 1560 cm^{-1} (2,5-substituted pyrrole), 1050 cm^{-1} (C—H vibration of 2,5-substituted pyrrole), and 920 and 800 cm^{-1} (C—H deformation of 2,5-substituted pyrrole); those of MMT clay were shown at 1040 cm^{-1} (Si—O), 600 cm^{-1} (Al—O), and 420 cm^{-1} (Mg—O).[21–23] As the loading of MMT clay was increased, the characteristic peaks of MMT clay bands became sharper in the FTIR spectra of PCN materials. Figure 2 showed the wide-angle powder X-ray diffraction patterns of organophilic clay and a series of PCN materials. There was a lack of any diffraction peak in 2θ = 2–10° as opposed to the diffraction peak at 2θ = 5.9° (d-spacing = 14.97 nm) for organophilic clay, indicating the possibility of having exfoliated silicate nanolayers of organophilic clay dispersed in polypyrrole matrix. When the organophilic clay loading increased up to 10 wt %, there appeared a diffraction peak at 2θ = 5.5° (d-spacing = 15.08 nm), implying an intercalated MMT clay nanolayer structure existed in the PPY matrix.

As shown in Figure 3, the TEM micrograph of PCN materials with 10 wt % clay loading showed that the nanocomposite had a mixed nanomorphology. Exfoliated layered structure such as individual silicate layers, along with two-, three-, and four-layer stacks, were found to be dispersed in PPY matrix. In addition, some larger intercalated tactoids can also be identified.

Corrosion protection properties of coatings

In this study, corrosion protection of sample-coated CRS coupons was evaluated based on the values of corrosion potential (E_{corr}), polarization resistance (R_p), corrosion current (i_{corr}), and corrosion rate (R_{corr}), as shown in Table I. The CRS coupon coated with PPY showed a higher E_{corr} value than the uncoated CRS, which was consistent with previous observations.[19,20] However, it exhibited a lower E_{corr} value than the specimen coated with PCN materials. For example, the PPYCL1-coated CRS had a high corrosion potential of ca. −474 mV at 30 min. Even after 5 h measurement, the potential remained at ca. −490 mV. Such an E_{corr} value indicated that the PPYCL1-coated CRS was much nobler toward the electrochemical corrosion

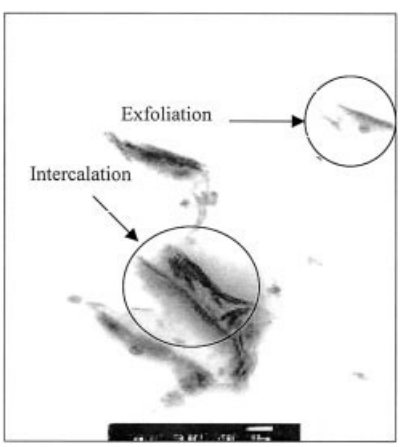

Figure 3 TEM of PPYCL10: with exfoliated single, double, and triple layers and a multilayer tactoid.

TABLE I
Relations of the composition of soluble electronically conductive polypyrrole (PPY)-MMT clay nonocomposite materials with the E_{corr}, R_p, i_{corr} and R_{corr} measured from electrochemical methods.

Compound code	Feed composition (wt %)		Inorganic content found in product[a] (wt %)	Electrochemical corrosion measurements[b]			
	Polypyrrole	MMT		E_{corr} (mV)	R_p (KΩ × cm^2)	I_{corr} (μA/cm^2)	R_{corr} (MPY)
Bare	—	—	—	−641	0.80	44.4	86.140
PPY	100	0	0	−546	17.96	2.75	0.064
PPYCL1	99	1	2.3	−474	24.51	1.87	0.044
PPYCL3	97	3	5.6	−470	50.43	0.87	0.020
PPYCL5	95	5	8.0	−421	68.71	0.54	0.013
PPYCL10	90	10	22.1	−351	120.38	0.02	0.001

[a] As determined from TGA measurements.
[b] A saturated calomel electrode was employed as the reference electrode.
[c] As measured by a digimatic micrometer.

compared to PPY. The PPYCL1-coated CRS showed a polarization resistance (R_p) value of 2.45×10^4 Ω/cm^2 in 5 wt % NaCl, which was about two orders of magnitude greater than the bare exposed CRS.

The Tafel plots for (a) bare, (b) PPY-coated, (c) PPYCL1-coated, and (d) PPYCL5-coated CRS were shown in Figure 4. For example, the corrosion current (i_{corr}) of PPYCL1-coated CRS was ca. 1.87 μA/cm^2, which corresponded to a corrosion rate (R_{corr}) of ca. 0.044 MPY (Table I). Electrochemical corrosion current values of PCN materials as coatings on CRS were found to decrease gradually with a further increase in clay loading. Furthermore, visual observation of the corrosion products clearly revealed that the PCN samples exhibiting corrosion protection had a grayish oxide layer form over the bare exposed CRS surface, similar to what was observed by Wessling under the polyaniline dispersion coatings on steel.[17] Advanced corrosion protection effect of polypyrrole–clay nanocomposite materials compared to pristine polypyrrole might have resulted from dispersing silicate nanolayers of clay in polypyrrole matrix to increase the tortuosity of the diffusion pathway of oxygen gas and H_2O vapor.[21,23]

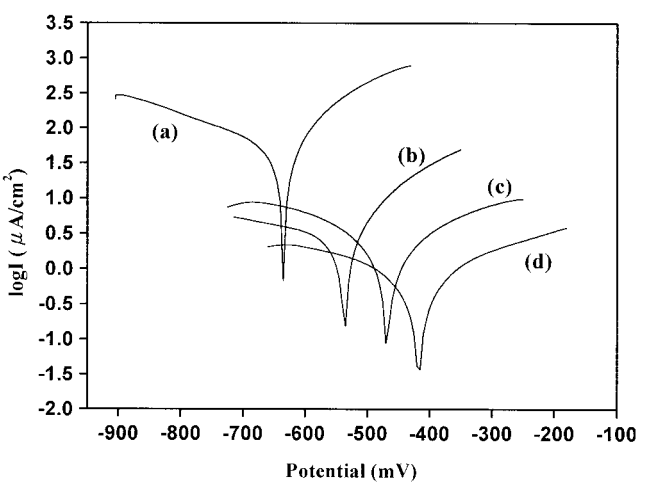

Figure 4 Tafel plots for (a) uncoated, (b) PPY-coated, (c) PPYCL1-coated, (d) PPYCL5-coated CRS measured in 5 wt % NaCl aqueous solution.

Thermal properties and electrical conductivity of fine powders

Figure 5 showed typical TGA curves of the PCN materials as well as that of polypyrrole, as measured under an air atmosphere. In general, there appeared to be several stages of weight loss starting at ~ 270°C and ending at 900°C, which might correspond to the degradation of the intercalating agent followed by the structural decomposition of the polymers. According to the published reports on polymer–clay nanocomposite materials, the unparalleled ability of smectite clays was found to boost the thermal stability of polymers.[3] Evidently, the onset of the thermal decomposition of those nanocomposites shifted slightly toward the higher temperature range than that of pristine PPY, which confirmed the enhancement of thermal stability of intercalated polymer.[22–23] After ~ 700°C, the curve all became flat and mainly the inorganic residue (i.e., Al_2O_3, MgO, SiO_2) remained. From the amounts of the residue at 700°C, the inorganic contents in the original PCN materials can be obtained, which were significantly higher than the values calculated from the feed composition. The calculated inorganic contents tend to be lower than those determined from TGA probably because of low yield of PPY prepared from pyrrole monomers in PCN materials.

Jeong et al.[26] reported that the glass transition temperature (T_g) of the PPY-ClO_4 film is approximately 268°C. Truong et al.[25] reported that the T_g of PPY-ClO_4 was approximately 155°C. In this study, we found that the T_g of PPY-DBSA is around 103°C. We also found from DSC measurements that the incorporation of MMT clay into PPY resulted in an increase in the T_g (heating scan) relative to pure PPY, as shown in Figure 6. This was tentatively associated with the confinement of the intercalated polymer chains within the

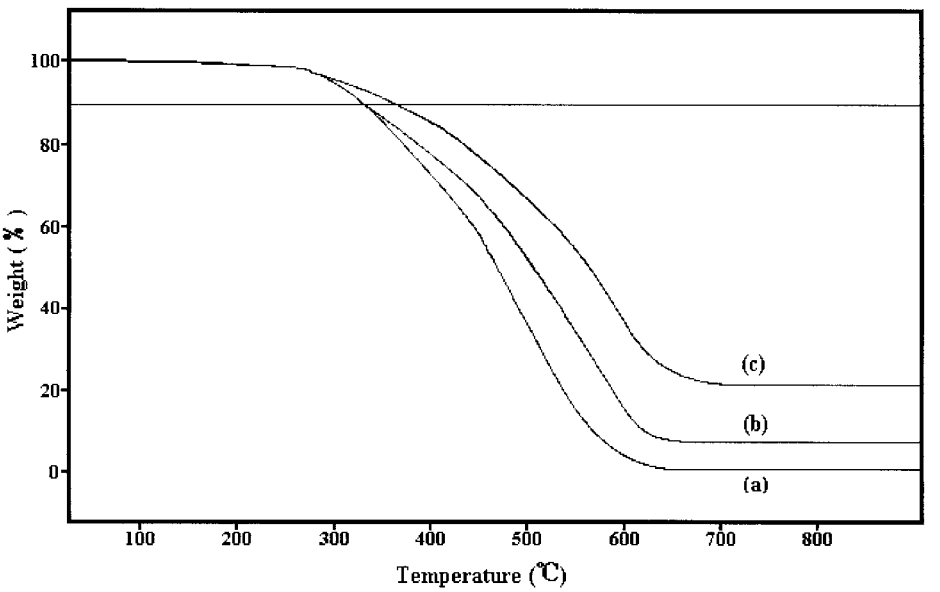

Figure 5 TGA curves of (a) PPY, (b) PPYCL5, (c) PPYCL10.

clay galleries that prevent the segmental motions of the polymer chains.[23] As the loading of MMT clay was increased, the T_g of PCN materials became higher. For the electronic property studies, the electrical conductivity of all the PCN materials in the form of a powder-pressed pellet was found slightly smaller than that of pristine PPY, as shown in Figure 7. This was expected because the MMT component was not electronically conductive and the incorporation of MMT clay platelets into PPY matrix contributed to a smaller molecular weight, leading to a lower electrical conductivity.[22]

Viscosity and UV-visible spectra of PPY and PCN materials

Viscosity of various polymer samples was obtained by viscometry analysis[28] with *m*-cresol as solvent, as shown in Figure 8. Viscosity of PPY existing in PCN materials was found significantly lower than that of the pristine PPY, indicating the structurally restricted polypyrrole polymerization conditions in the intragallery region of the MMT clay.[21,23] The lower value of viscosity of PCN materials corresponded to a smaller molecular weight of PPY existing in PCN materials. Furthermore, for the optical property studies, it can be easily found that the absorption band at 944 nm and a shoulder peak at 720 nm were presented in the UV-visible spectra of PPY doped with DBSA.[29] It was interesting to find that the peak position of π-π^* absorption is 427 nm for the PPYCL5 in *m*-cresol solution, which was between 421 nm for the PPYCL10 and 430 nm for PPY in the same solvent, as shown in Figure 9. Obviously, UV-visible spectra of PCN materials displayed a blue shift compared to the pristine PPY material, reflecting to a decreased conjugated

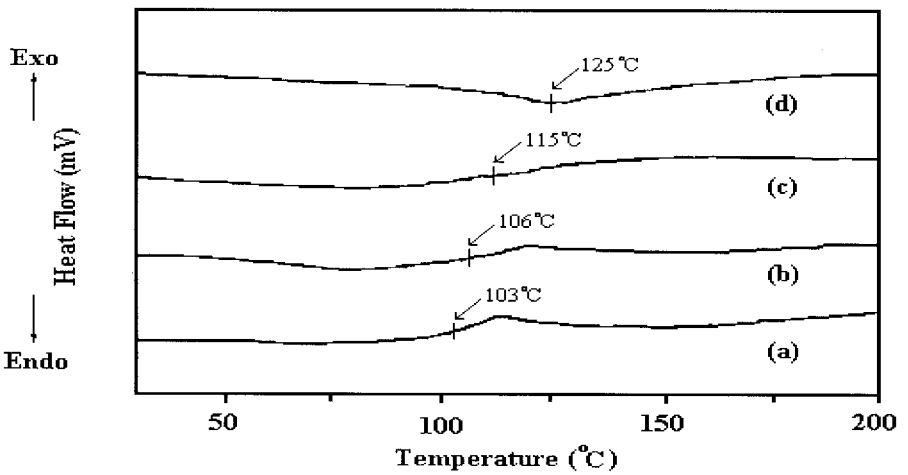

Figure 6 DSC curves of (a) PPY, (b) PPYCL1, (b)PPYCL3, (d) PPYCL10.

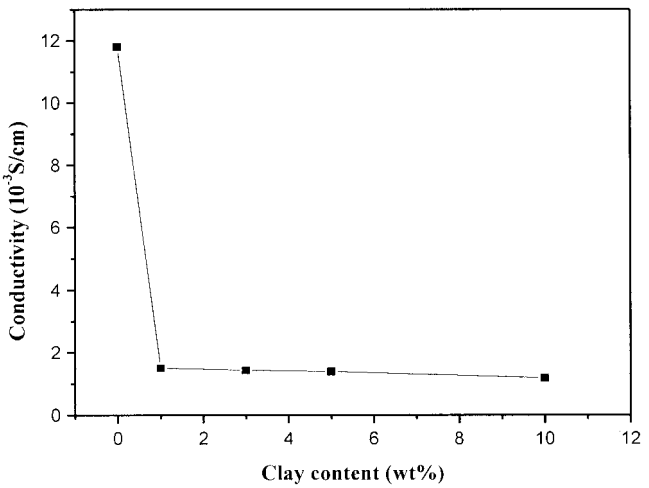

Figure 7 Relationships between electrical conductivity and clay loading as obtained from four-probe technique measurements.

chain length of PPY in PCN materials, which was consistent with the previous results obtained from viscometry analysis studies.

Heterogeneous nucleating effect of clay platelets in PPY matrix (SEM, XRD)

Heterogeneous nucleating agents had been used in industry to enhance optical properties (such as transparency) and mechanical properties (such as impact resistance, tensile strength, and elongation at break). These special properties can be achieved effectively by introducing a heterogeneous nucleating agent to increase the nucleation density, resulting in spherulite size reduction.[30–32] The dispersed clay platelets functioning as nucleating agent had been reported to significantly influence the crystallization and polymorphism of polyesters and polyamides.[33] Ke et al. found a threefold increase in the crystallization rate of PET containing 5 wt % dispersed clay relative to that of pristine PET.[33a] The increased crystallization rate was related to a nucleating effect of the clay platelets.

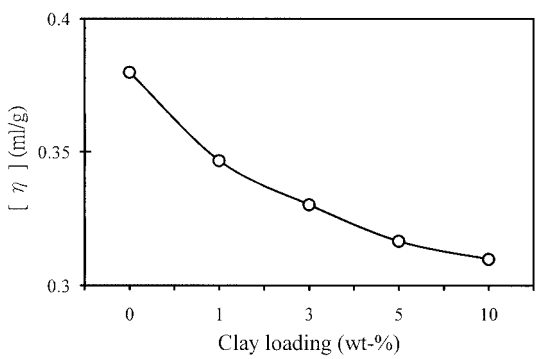

Figure 8 Relationships between viscosity and clay loading as obtained from viscometry measurements.

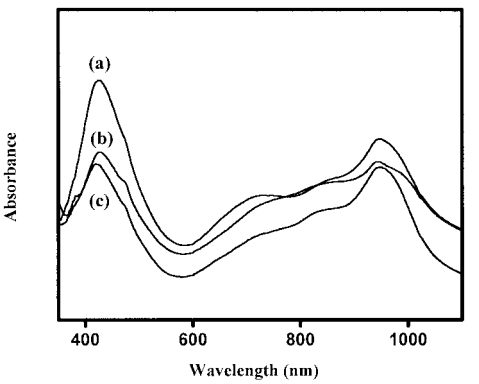

Figure 9 UV-visible absorption spectra of (a) PPY, (b) PPYCL5, (c) PPYCL10.

Similar results were also found by Jimenez et al. for polyamide and polyester systems.[33b] Furthermore, the presence of clay platelets affected changes in the polymorphic composition of Nylon 6, relative to the pure samples without clay. Barber and Moore reported that the incorporation of clay into PET resulted in a large increase in the crystallization temperature relative to pure PET.[34] In this study, the heterogeneous nucleating effect of MMT clay platelets was also found in PPY matrix based on the examination of wide-angle powder XRD patterns, as shown in Figure 10. The XRD pattern of PCN materials (e.g., PPYCL10) was revealed, increasing sharper crystalline peaks around 2θ = 18.6°, 20.2°, 22.0°, and 27.5°, indicating that the dispersing of MMT clay platelets into PPY matrix led to an effective increase in the polymeric crystallinity resulted from the heterogeneous nucleating effect of layered silicate existing in polymer matrix. On the other hand, the morphological topology of as-synthesized materials can also be studied by SEM. The micrographs of PPY and PPYCL10 at 10K magnification were presented in Figure 11. PPY [Fig. 11(a)] showed loose-packing morphological image, reflecting a low crystallinity of pristine electronically conductive PPY matrix. However, the SEM micrograph of PPYCL10 [Fig. 11(b)] showed wealthy and much larger compact-packing of crystalline domains, corresponding to a polymer matrix with higher crystallinity, which was consistent with the results obtained from the wide-angle powder X-ray diffraction pattern studies.

CONCLUSIONS

In this article, we found that electronically conductive PCN materials at low clay loading showed an advanced corrosion protection effect compared to pristine PPY through a series of electrochemical measurements including corrosion potential, polarization resistance, and corrosion current on CRS in 5 wt % aqueous NaCl electrolyte. The as-synthesized PCN materials were characterized by FTIR, wide-angle

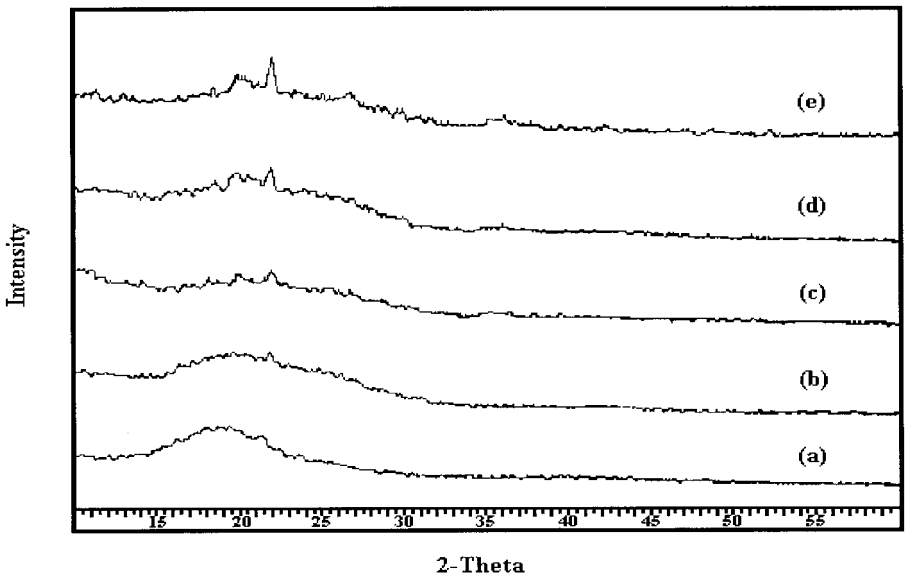

Figure 10 Powder X-ray diffraction patterns ranging from $2\theta = 10°$ to 60° of (a) PPY, (b) PPYCL1, (c) PPYCL3, (d) PPYCL5, (e) PPYCL10.

powder X-ray diffraction, and TEM. Effects of the material composition on the thermal stability, optical properties, and electrical conductivity of pristine PPY along with PCN materials, in the form of fine powder and powder-pressed pellet, were also studied by DSC, TGA, UV-visible, and four-point probe technique, respectively. The incorporation of nanolayers of MMT clay in electronically conductive PPY matrix resulted in a slight increase in thermal decomposition temperature (T_d) based on the TGA studies. Dispersed nanolayers of MMT clays in electronically conductive PPY led to a significant increase of T_g based on the DSC results. This was tentatively associated with the confinement of the intercalated polymer chains within the clay galleries that prevent the segmental motions of the polymer chains. Electrical conductivity of all the PCN materials in the form of a powder-pressed pellet was found to be slightly smaller than that of pristine PPY. This was expected because the MMT component is not electronically conductive and the incorporating of MMT clay into PPY matrix contributes to a smaller molecular weight, reflecting a lower electrical conductivity. Viscosity of extracted PPY was found significantly lower than that of the pristine PPY, indicating the structurally restricted polymerization conditions in the intragallery region of the MMT clay. UV-visible absorption spectra of PCN materials displayed a blue shift compared to the pristine PPY material, reflecting a decreased conjugated chain length of PPY in PCN materials compared to pristine polymer, which was consistent with the results obtained from viscometry analysis studies. The effectively heterogeneous nucleating effect of MMT clay platelets in PPY matrix was investigated by wide-angle powder XRD and SEM.

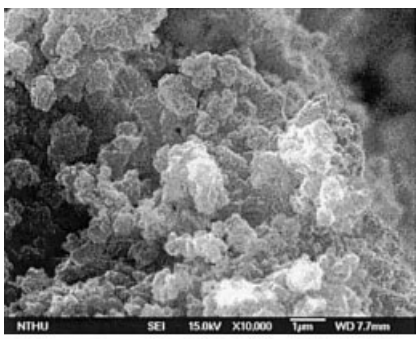

(a) PPY

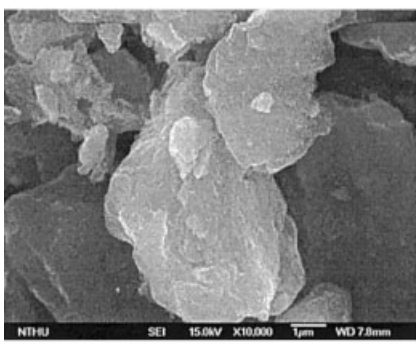

(b) PPYCL10

Figure 11 Scanning electron micrographs of PPY-MMT nanocomposite materials at 10K magnification: (a) PPY, (b) PPYCL10.

The financial support of this research by the NSC 90-2113M-033-010 is gratefully acknowledged.

References

1. Pinnavaia, T. J. Science 1983, 220, 365.
2. Lan, T.; Kaviratna, P. D.; Pinnavaia, T. J. Chem Mater 1994, 6, 573.
3. Tyan, H.-L.; Liu, Y.-C.; Wei, K.-H. Chem Mater 1999, 11,1942.
4. Wang, Z.; Pinnavaia, T. J. Chem Mater 1998, 10, 3769.
5. Gilman, J. W.; Jackson, C. L.; Morgan, A. B.; Hayyis, R., Jr.; Manias, E.; Giannelis, E. P.; Wuthenow, M.; Hilton, D.; Phillips, S. H. Chem Mater 2000, 12, 1866.
6. Biswas, M.; Ray, S. S. J Appl Polym Sci 2000, 77, 2948.
7. Wu, C.-G.; DeGroot, D. C.; Marcy, H. O.; Schindler, J. L.; Kannewurf, C. R.; Liu, Y.-J.; Hirpo, W.; Kanatzidis, M. G. Chem Mater 1996, 8, 1992.
8. Wang, L.; Brazis, P.; Rocci, M.; Kannewurf, C. R.; Kanatzidis, M. G. Chem Mater 1998, 10, 3298.
9. Chao, K.-J.; Ho, S.-Y.; Chang, T.-C. U.S. Pat. 5,340,500, 1994.
10. Giannelis, E.; Mehrota, V. U.S. Pat. 5,032,547, 1991.
11. Choi, H. J.; Kim, J. W.; Kim, S. G.; Kim, B. H.; Joo, J. Polym Mater Sci Eng 2000, 82, 245.
12. Wu, Q.; Xue, Z.; Qi, Z.; Wang, F. Polymer 2000, 41, 2029.
13. Deberry, D. W. J Electrochem Soc 1985, 132, 1027.
14. Wessling, B. Synth Met 1997, 85, 1318.
15. Elsenbaumer, R. L.; Lu, W. K.; Wessling, B. International Conference of Synthetic Metals; Seoul, Korea; Abstract No. APL-(POL)1-2, 1994.
16. Wrobleski, D. A.; Benicewicz, B. C.; Thompson, K. G.; Byran, C. J. Polym Prepr (Am Chem Soc, Div Polym Chem) 1994, 35 (1), 265.
17. Wessling, B. Adv Mater 1994, 6, 226.
18. Wei, Y.; Wang, J.; Jia, X.; Yeh, J.-M.; Spellane, P. Polymer 1995 36, 4535.
19. Krstajic, N. V.; Grgur, B. N.; Jovanovic, S. M.; Vojnovic, M. V. Electrochim Acta 1997, 42 (11), 1695.
20. Troch-Nagels, G.; Winand, R.; Weymeersch, A.; Renard, L. J Appl Electrochem 1992, 22, 756.
21. Yeh, J.-M.; Liou, S.-J.; Lai, C.-Y.; Wu, P.-C.; Tsai, T.-Y. Chem Mater 2001, 13, 1131.
22. Yeh, J.-M.; Chen, C.-L.; Chen, Y.-C.; Ma, C.-Y; Lee, K.-R.; Wei, Y.; Li, S. Polymer 2002, 43, 2729.
23. Yeh, J.-M.; Liou, S.-J.; Lin, C.-Y.; Cheng, C.-Y.; Chang, Y.-W.; Lee, K.-R. Chem Mater 2002, 14, 154.
24. Oriakhi, C. O.; Lerner, M. M. Mater Res Bull 1995, 30 (6), 723.
25. SinhaRay, S.; Biswas, M. Mater Res Bull 1999, 34 (8), 1187.
26. Jeong, R. A.; Lee, G.-J.; Kim, H.-S.; Ahn, K.; Lee, K.; Kim, K.-H. Synth Met 1998, 98, 9.
27. Truong, V. T.; Ennis, B. C.; Forsyth, M. Polymer 1995, 36 (10), 1993.
28. Arizzi, S.; Suter, U. W. Polym Mater Sci Eng Prepr 1989, 61, 481.
29. Lee, J. Y.; Kim, D. Y.; Kim, C. Y. Synth Met 1995, 74, 103.
30. Khanna, Y. P.; Reimschuessel, A. C.; Banjerie, A.; Altman, C. Polym Eng Sci 1988, 28, 1600.
31. Khanna, Y. P.; Reimschuessel, A. C. J Appl Polym Sci 1988, 35, 2259.
32. Muellerleile, J. T.; Freeman, J. J. J Appl Polym Sci 1994, 54, 135.
33. (a) Ke, Y.; Long, C.; Qi, Z. J Appl Sci 1999, 40, 4877; (b) Jimenez, G.; Ogata, N.; Kawai, H.; Ogihara, T. J Appl Polym Sci 1997, 64, 2211; (c) Boykin, T. L.; Moore, R. B. Polym Prepr 1998, 39, 393.
34. Barber, G. D.; Moore, R. B. Polym Mater Sci Eng 2000, 82, 241.